

# Macrocyclic Binucleating $\beta$ -Diketiminato Ligands and Their Lithium, Aluminum, and Zinc Complexes

Javier Vela, Liwei Zhu, Christine J. Flaschenriem, William W. Brennessel, Rene J. Lachicotte, and Patrick L. Holland\*

Department of Chemistry, University of Rochester, Rochester, New York 14627

Received January 9, 2007

The incorporation of rigid aromatic linkers into  $\beta$ -diketiminato ligands creates a binucleating scaffold that holds two metals near each other. This paper discloses the synthesis, characterization, and reactivity of  $m\text{Bin}^{2-}$ , which has a meta-substituted xylylene spacer, and  $p\text{Bin}^{2-}$ , which has a para-substituted xylylene spacer. Lithium, aluminum, and zinc complexes of each ligand have been isolated, and in some cases characterized by X-ray crystallography. The lithium complexes are coordinated to solvent-derived THF ligands, while the zinc and aluminum complexes have alkyl ligands. Complexes of the  $m\text{Bin}^{2-}$  ligand have an anti conformation in which the metals are on opposite sides of the macrocycle, while  $p\text{Bin}^{2-}$  complexes prefer a syn conformation. The  $^1\text{H}$  NMR spectra of the complexes demonstrate that the conformations interconvert rapidly in the lithium complexes and less rapidly in the zinc and aluminum complexes.

## Introduction

Anionic diimine ligands derived from  $\beta$ -diketones, termed " $\beta$ -diketiminates", have served as useful Schiff base ligands in coordination chemistry for decades.<sup>1</sup> Because they form a six-membered ring with the metal, coordinate through strongly donating nitrogen atoms, and have an overall negative charge, they are excellent chelating ligands, despite the fact that they are not always inert to ligand-based reactions.<sup>2</sup> Bulky  $\beta$ -diketiminato complexes have been especially popular recently and have found use in a number of applications, including catalysts for polymerization,<sup>3</sup> alkane and arene activation,<sup>4</sup> hydroamination,<sup>5</sup>

carboamination,<sup>6</sup> and hydrodefluorination.<sup>7</sup> They have also been used for stabilization of CVD precursors,<sup>8</sup> reactive metal–ligand multiple bonds,<sup>9–12</sup> metal–metal bonds,<sup>13</sup> and copper–dioxygen complexes.<sup>14</sup>

One of our research goals is the study of complexes with multiple iron atoms held by  $\beta$ -diketiminato ligands.<sup>15</sup> These perform cooperative multimetallic reactions of relevance to the mechanism of iron–molybdenum nitrogenase, which has a Fe7–

\* To whom correspondence should be addressed. E-mail: holland@chem.rochester.edu.

(1) (a) Everett, G. W., Jr.; Holm, R. H. *J. Am. Chem. Soc.* **1965**, *87*, 2117–2127. (b) Bourget-Merle, L.; Lappert, M. F.; Severn, J. R. *Chem. Rev.* **2002**, *102*, 3031–3066.

(2) (a) Radzewich, C. E.; Coles, M. P.; Jordan, R. F. *J. Am. Chem. Soc.* **1998**, *120*, 9384–9385. (b) Fekl, U.; Kaminsky, W.; Goldberg, K. I. *J. Am. Chem. Soc.* **2001**, *123*, 6423–6424. (c) Yokota, S.; Tachi, Y.; Itoh, S. *Inorg. Chem.* **2002**, *41*, 1342–1344. (d) Cope-Eatough, E. K.; Mair, F. S.; Pritchard, R. G.; Warren, J. E.; Woods, R. J. *Polyhedron* **2003**, *22*, 1447–1454. (e) Harder, S. *Angew. Chem., Int. Ed.* **2003**, *42*, 3430–3434. (f) Basuli, F.; Huffman, J. C.; Mendiola, D. J. *Inorg. Chem.* **2003**, *42*, 8003–8010. (g) Basuli, F.; Bailey, B. C.; Brown, D.; Tomaszewski, J.; Huffman, J. C.; Baik, M.-H.; Mendiola, D. J. *J. Am. Chem. Soc.* **2004**, *126*, 10506–10507. (h) Gregory, E. A.; Lachicotte, R. J.; Holland, P. L. *Organometallics* **2005**, *24*, 1803–1805. (i) Zhu, H.; Chai, J.; Jancik, V.; Roesky, H. W.; Merrill, W. A.; Power, P. P. *J. Am. Chem. Soc.* **2005**, *127*, 10170–10171. (j) Reynolds, A. M.; Lewis, E. A.; Aboeella, N. W.; Tolman, W. B. *Chem. Commun.* **2005**, 2014–2016. (k) Basuli, F.; Huffman, J. C.; Mendiola, D. J. *Inorg. Chim. Acta* **2007**, *360*, 246–254.

(3) (a) Cheng, M.; Lobkovsky, E. B.; Coates, G. W. *J. Am. Chem. Soc.* **1998**, *120*, 11018–11019. (b) Vollmerhaus, R.; Rahim, M.; Tomaszewski, R.; Xin, S.; Taylor, N. J.; Collins, S. *Organometallics* **2000**, *19*, 2161–2169. (c) Chisholm, M. H.; Huffman, J. C.; Phomphrai, K. *Dalton Trans.* **2001**, 222–224. (d) Chamberlain, B. M.; Cheng, M.; Moore, D. R.; Oviatt, T. M.; Lobkovsky, E. B.; Coates, G. W. *J. Am. Chem. Soc.* **2001**, *123*, 3229–3238. (e) Cheng, M.; Moore, D. R.; Reczek, J. J.; Chamberlain, B. M.; Lobkovsky, E. B.; Coates, G. W. *J. Am. Chem. Soc.* **2001**, *123*, 8738–8749. (f) Gibson, V. C.; Marshall, E. L.; Navarro-Llobet, D.; White, A. J. P.; Williams, D. J. *Dalton Trans.* **2002**, 4321–4322. (g) Moore, D. R.; Cheng, M.; Lobkovsky, E. B.; Coates, G. W. *J. Am. Chem. Soc.* **2003**, *125*, 11911–11924. (h) Byrne, C. M.; Allen, S. D.; Lobkovsky, E. B.; Coates, G. W. *J. Am. Chem. Soc.* **2004**, *126*, 11404–11405. (i) Chisholm, M. H.; Gallucci, J. C.; Phomphrai, K. *Inorg. Chem.* **2005**, *44*, 8004–8010.

(4) (a) Fekl, U.; Kaminsky, W.; Goldberg, K. I. *J. Am. Chem. Soc.* **2003**, *125*, 15286–15287. (b) Bernskoetter, W. H.; Lobkovsky, E.; Chirik, P. J. *Chem. Commun.* **2004**, 764–765. (c) Bernskoetter, W. H.; Lobkovsky, E.; Chirik, P. J. *Organometallics* **2005**, *24*, 4367–4373.

(5) Crimmin, M. R.; Casely, I. J.; Hill, M. S. *J. Am. Chem. Soc.* **2005**, *127*, 2042–2043.

(6) Zhao, G.; Basuli, F.; Kilgore, U. J.; Fan, H.; Aneetha, H.; Huffman, J. C.; Wu, G.; Mendiola, D. J. *J. Am. Chem. Soc.* **2006**, *128*, 13575–13585.

(7) Vela, J.; Smith, J. M.; Yu, Y.; Ketterer, N. A.; Flaschenriem, C. J.; Lachicotte, R. J.; Holland, P. L. *J. Am. Chem. Soc.* **2005**, *127*, 7857–7870.

(8) Park, K.-H.; Bradley, A. Z.; Thompson, J. S.; Marshall, W. J. *Inorg. Chem.* **2006**, *45*, 8480–8482.

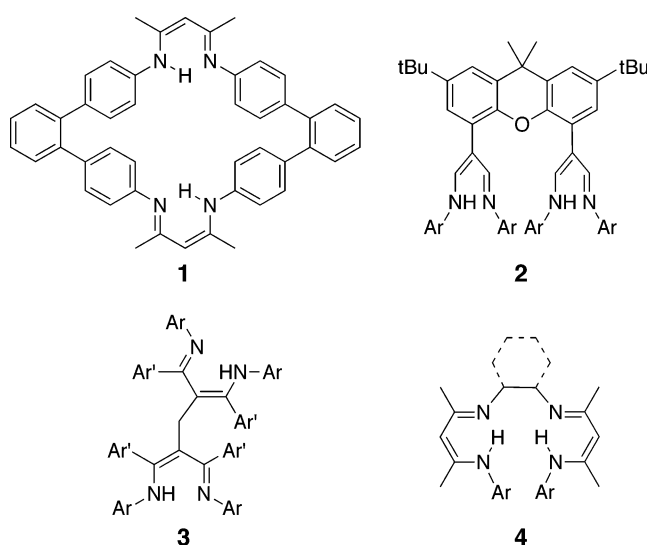
(9) (a) Dai, X.; Warren, T. H. *J. Am. Chem. Soc.* **2004**, *126*, 10085–10094. (b) Dai, X.; Kapoor, P.; Warren, T. H. *J. Am. Chem. Soc.* **2004**, *126*, 4798–4799. (c) Badiel, Y. M.; Krishnaswamy, A.; Melzer, M. M.; Warren, T. H. *J. Am. Chem. Soc.* **2006**, *128*, 15056–15057. (d) Kogut, E.; Wiencko, H. L.; Zhang, L.; Cordeau, D. E.; Warren, T. H. *J. Am. Chem. Soc.* **2005**, *127*, 11248–11249.

(10) (a) Basuli, F.; Tomaszewski, J.; Huffman, J. C.; Mendiola, D. J. *J. Am. Chem. Soc.* **2003**, *125*, 10170–10171. (b) Basuli, F.; Bailey, B. C.; Tomaszewski, J.; Huffman, J. C.; Mendiola, D. J. *J. Am. Chem. Soc.* **2003**, *125*, 6052–6053. (c) Basuli, F.; Bailey, B. C.; Brown, D.; Tomaszewski, J.; Huffman, J. C.; Baik, M.-H.; Mendiola, D. J. *J. Am. Chem. Soc.* **2004**, *126*, 10506–10507. (d) Basuli, F.; Kilgore, U. J.; Brown, D.; Huffman, J. C.; Mendiola, D. J. *Organometallics* **2004**, *23*, 6166–6175. (e) Basuli, F.; Kilgore, U. J.; Hu, X.; Meyer, K.; Pink, M.; Huffman, J. C.; Mendiola, D. J. *Angew. Chem., Int. Ed.* **2004**, *43*, 3156–3159. (f) Basuli, F.; Bailey, B. C.; Huffman, J. C.; Mendiola, D. J. *Organometallics* **2005**, *24*, 3321–3334. (g) Basuli, F.; Clark, R. L.; Bailey, B. C.; Brown, D.; Huffman, J. C.; Mendiola, D. J. *Chem. Commun.* **2005**, 2250–2252. (h) Mendiola, D. J. *Acc. Chem. Res.* **2006**, *39*, 813–821.

(11) Eckert, N. A.; Vaddadi, S.; Stoian, S.; Lachicotte, R. J.; Cundari, T. R.; Holland, P. L. *Angew. Chem., Int. Ed.* **2006**, *45*, 6868–6871.

(12) (a) Hardman, N. J.; Cui, C.; Roesky, H. W.; Fink, W. H.; Power, P. P. *Angew. Chem., Int. Ed.* **2001**, *40*, 2172–2174. (b) Ding, Y.; Ma, Q.; Uson, I.; Roesky, H. W.; Noltemeyer, M.; Schmidt, H.-G. *J. Am. Chem. Soc.* **2002**, *124*, 8542–8543. (c) Zhu, H.; Chai, J.; Chandrasekhar, V.; Roesky, H. W.; Magull, J.; Vidovic, D.; Schmidt, H.-G.; Noltemeyer, M.; Power, P. P. *J. Am. Chem. Soc.* **2004**, *126*, 9472–9473.

Chart 1



Mo active site with  $\text{Fe}_2$  units at which  $\text{N}_2$  may be reduced.<sup>16</sup> In order to control the spatial relationship of the open coordination sites of two metals in a bimetallic complex,<sup>17</sup> it is reasonable to synthesize binucleating  $\beta$ -diketiminato ligands that can accommodate two metals. In addition to nitrogenase modeling, such ligands could be useful in manipulating other multimetallic reactions of  $\beta$ -diketiminato complexes.<sup>9,18</sup>

Ligands composed of two  $\beta$ -diketiminato units have received increasing attention in the literature. Lee and co-workers reported a macrocyclic ligand (**1**) (Chart 1) that consists of two  $\beta$ -diketiminato units rigidly held by an arene spacer.<sup>19</sup> They reported  $\text{Cu}_2$  and  $\text{Zn}_2$  salts of this ligand and incorporated alkyl substituents that are necessary for solubility.<sup>20</sup> Limberg has described a xanthene-bridged binucleating ligand with two

(13) (a) Chai, J.; Zhu, H.; Stueckl, A. C.; Roesky, H. W.; Magull, J.; Bencini, A.; Caneschi, A.; Gatteschi, D. *J. Am. Chem. Soc.* **2005**, *127*, 9201–9206. (b) Chai, J.; Zhu, H.; Stueckl, A. C.; Roesky, H. W.; Magull, J.; Bencini, A.; Caneschi, A.; Gatteschi, D. *J. Am. Chem. Soc.* **2005**, *127*, 9201. (c) Wang, Y.; Quillian, B.; Wei, P.; Wang, H.; Yang, X.-J.; Xie, Y.; King, R. B.; Schleyer, P. v. R.; Schaefer, H. F., III; Robinson, G. H. *J. Am. Chem. Soc.* **2005**, *127*, 11944–11945. (d) Hill, M. S.; Hitchcock, P. B.; Pongtavornpinyo, R. *Science* **2006**, *311*, 1904–1907.

(14) (a) Spencer, D. J. E.; Aboeella, N. W.; Reynolds, A. M.; Holland, P. L.; Tolman, W. B. *J. Am. Chem. Soc.* **2002**, *124*, 2108–2109. (b) Cramer, C. J.; Tolman, W. B.; Theopold, K. H.; Rheingold, A. L. *Proc. Nat. Acad. Sci. U.S.A.* **2003**, *100*, 3635–3640. (c) Aboeella, N. W.; Kryatov, S. V.; Gherman, B. F.; Brennessel, W. W.; Young, V. G., Jr.; Sarangi, R.; Rybak-Akimova, E. V.; Hodgson, K. O.; Hedman, B.; Solomon, E. I.; Cramer, C. J.; Tolman, W. B. *J. Am. Chem. Soc.* **2004**, *126*, 16896–16911. (d) Aboeella, N. W.; Gherman, B. F.; Hill, L. M. R.; York, J. T.; Holm, N.; Young, V. G.; Cramer, C. J.; Tolman, W. B. *J. Am. Chem. Soc.* **2006**, *128*, 3445–3458.

(15) (a) Smith, J. M.; Lachicotte, R. J.; Pittard, K. A.; Cundari, T. R.; Lukat-Rodgers, G.; Rodgers, K. R.; Holland, P. L. *J. Am. Chem. Soc.* **2001**, *123*, 9222–9223. (b) Vela, J.; Stoian, S.; Flaschenriem, C. J.; Münck, E.; Holland, P. L. *J. Am. Chem. Soc.* **2004**, *126*, 4522–4523. (c) Holland, P. L. *Can. J. Chem.* **2005**, *83*, 296–301. (d) Smith, J. M.; Sadique, A. R.; Cundari, T. R.; Rodgers, K. R.; Lukat-Rodgers, G.; Lachicotte, R. J.; Flaschenriem, C. J.; Vela, J.; Holland, P. L. *J. Am. Chem. Soc.* **2006**, *128*, 756–769. (e) Stoian, S. A.; Vela, J.; Smith, J. M.; Sadique, A. R.; Holland, P. L.; Münck, E.; Bominaar, E. L. *J. Am. Chem. Soc.* **2006**, *128*, 10181–10192.

(16) (a) Christiansen, J.; Dean, D. R.; Seefeldt, L. C. *Annu. Rev. Plant Physiol. Plant Mol. Biol.* **2001**, *52*, 269–295. (b) Seefeldt, L. C.; Dance, I. G.; Dean, D. R. *Biochemistry* **2004**, *43*, 1401–1409. (c) Dos Santos, P. C.; Igarashi, R. Y.; Lee, H.-I.; Hoffman, B. M.; Seefeldt, L. C.; Dean, D. R. *Acc. Chem. Res.* **2005**, *38*, 208–214.

(17) Gavrilova, A. L.; Bosnich, B. *Chem. Rev.* **2004**, *104*, 349–383.

(18) Moore, D. R.; Cheng, M.; Lobkovsky, E. B.; Coates, G. W. *J. Am. Chem. Soc.* **2003**, *125*, 11911–11924.

(19) Lee, S. Y.; Na, S. J.; Kwon, H. Y.; Lee, B. Y.; Kang, S. O. *Organometallics* **2004**, *23*, 5382–5385.

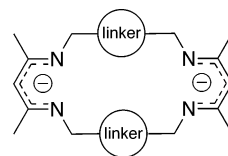


**Figure 1.** Template for easily synthesized binucleating ligands Bin, based on the conceptual condensation of 2,4-pentanedione with aromatic xylylenediamines.

parallel binding sites (**2**).<sup>21</sup> Lappert has created binucleating  $\beta$ -diketiminates that are linked through the backbone (**3**).<sup>22</sup> Other ligands that give two adjacent metal-binding sites similar to  $\beta$ -diketiminates have been reported.<sup>23</sup> Ligands such as tetraazaannulenes with two-carbon linkers typically coordinate to a single metal;<sup>24</sup> for example, **4** gives mononuclear complexes.<sup>25</sup> However, even tetraazaannulenes can act as binucleating ligands under the appropriate conditions.<sup>26</sup>

Our strategy was based on ease of synthesis, as well as the use of a rigid, tunable linker that holds two  $\beta$ -diketiminato units far enough apart that they cannot both coordinate to the same metal but close enough that they can engage in cooperative reactions. A simple way to do this is by linking the arene groups of the  $\beta$ -diketiminato to give the ligand scaffold shown in Figure 1.<sup>19</sup> Here, we describe the initial coordination chemistry of two new ligands of this type. X-ray crystallography and NMR spectroscopy elucidate important features of the conformations of the ligands, giving insight into their suitability for bimetallic reactions.

## Results and Discussion

### Synthesis and Characterization of Protonated Ligands.

Condensation of the ethylene glycol monoketal of 2,4-pentanedione with 1 equiv of either *m*-xylylenediamine or *p*-xylylenediamine gives the desired ligands (Scheme 1). This condensation is preferable to the typical acid-catalyzed condensations of diketones, because no acid catalyst is required in the ligand synthesis, and the latter method gave mixtures of products. Using the method in Scheme 1, the ligands mBinH<sub>2</sub> and pBinH<sub>2</sub> are obtained in 89% and 59% yields, respectively. In this notation, we refer to ligands as mBin<sup>2-</sup> for the binucleating ligand with the 1,3-substituted arene linker and pBin<sup>2-</sup> for the binucleating ligand with the 1,4-substituted arene linker. In general, mBin-derived compounds are somewhat more soluble than the pBin-derived analogues.

The <sup>1</sup>H NMR spectra of mBinH<sub>2</sub> and pBinH<sub>2</sub> each show a singlet that integrates to two protons at 4.6–4.7 ppm and another singlet that integrates to two protons at 11–12 ppm, indicating that one imine on each side exists as the enamine tautomer (Figure 2). This tautomer is commonly observed in  $\beta$ -diketiminates, because the N–H proton of the enamine has a stabilizing

(20) Lee, B. Y.; Kwon, H. Y.; Lee, S. Y.; Na, S. J.; Han, S.; Yun, H.; Lee, H.; Park, Y.-W. *J. Am. Chem. Soc.* **2005**, *127*, 3031–3037.

(21) Pilz, M. F.; Limberg, C.; Ziemer, B. *J. Org. Chem.* **2006**, *71*, 4559–4564.

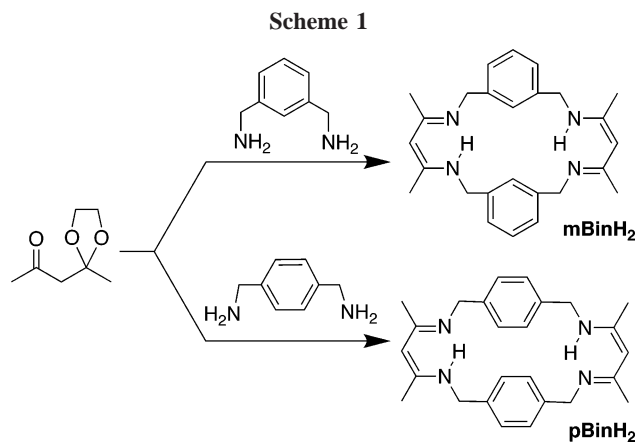
(22) Bourget-Merle, L.; Hitchcock, P. B.; Lappert, M. F. *J. Organomet. Chem.* **2004**, *689*, 4357.

(23) (a) Allen, S. D.; Moore, D. R.; Lobkovsky, E. B.; Coates, G. W. *J. Organomet. Chem.* **2003**, *683*, 137–148. (b) Hebden, T. J.; Brennessel, W. W.; Flaschenriem, C. J.; Holland, P. L. *Dalton Trans.* **2006**, 3855–3857.

(24) Busch, D. H. *Acc. Chem. Res.* **1978**, *11*, 392–400.

(25) (a) Vitanova, D. V.; Hampel, F.; Hultzsich, K. C. *J. Organomet. Chem.* **2005**, *690*, 5182–5197. (b) Vitanova, D. V.; Hampel, F.; Hultzsich, K. C. *Dalton Trans.* **2005**, 1565–1566.

(26) Fandos, R.; Walter, M. D.; Kazhdan, D.; Andersen, R. A. *Organometallics* **2006**, *25*, 3706–3715 and references therein.



hydrogen bond with the lone pair of the nearby imine (this hydrogen bond results in the downfield shift of the N–H proton).<sup>1</sup> The infrared spectrum of each compound shows a band in the 3200–3300  $\text{cm}^{-1}$  range that corresponds to stretching of this N–H bond. Despite the inherent asymmetry of the enamine/imine tautomer, the  $^1\text{H}$  NMR spectrum is consistent with  $D_{2h}$  symmetry, in which there are effectively three mirror planes and  $C_2$  axes splitting the molecule. This observation implies that the enamine/imine tautomers are equilibrating more quickly than the NMR time scale.

The solid-state structure of  $\text{pBinH}_2$  from X-ray crystallography is of sufficient quality to locate and refine the positions of the N–H hydrogen atoms, showing that the tautomer present in the crystal has both N–H protons on the same side (Figure 3). The location of these protons is consistent with the bond localization in the NCCC backbone (Table 1), where for example N(1)–C(1) is about 0.04 Å shorter than N(2)–C(3). (However, as shown in the previous paragraph, the tautomers exchange rapidly in  $\text{CDCl}_3$  solution.) The bridging *p*-xylylene rings are nearly parallel to the plane of the large macrocycle (dihedral angles of 2.62(2) and 10.85(2)°) in the solid-state structure, but these must be rapidly spinning around the C(aryl)–C(methylene) bonds in solution to explain the equivalence of all four aryl protons in the  $^1\text{H}$  NMR spectrum.

**Lithium Complexes of the Binucleating Ligands.** Addition of 2 equiv of *n*-butyllithium to solutions of the ligands in dry, degassed THF gives the lithium complexes  $\text{mBinLi}_2(\text{THF})_2$  and  $\text{pBinLi}_2(\text{THF})_3$ . The numbers of coordinated THF molecules in the formulas come from the integration of the signals for the THF protons in the  $^1\text{H}$  NMR spectra of  $\text{C}_6\text{D}_6$  solutions. The

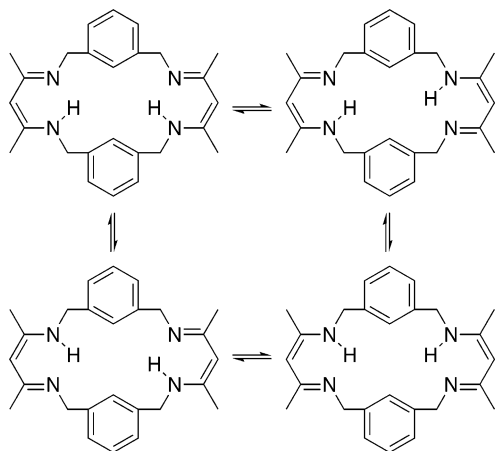


**Figure 2.** Tautomers of  $\text{mBinH}_2$ . The analogous tautomers are present for  $\text{pBinH}_2$ .

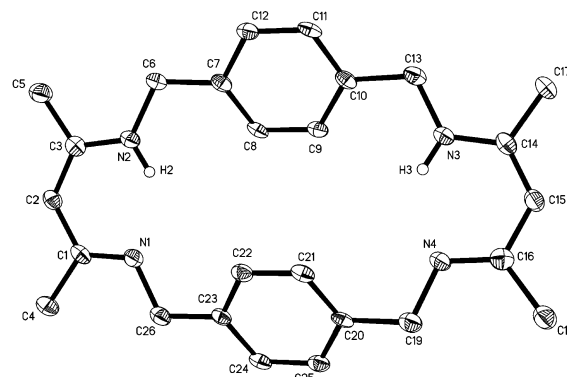


**Figure 3.** Thermal ellipsoid plot of  $\text{pBinH}_2$  showing 50% probability ellipsoids. Carbon-bound hydrogen atoms have been omitted for clarity.

**Table 1.** Selected Bond Lengths (Å) and Angles (deg) for  $\text{pBinH}_2$

C3–C5	1.497(3)	C14–C17	1.507(3)
C2–C3	1.380(3)	C14–C15	1.370(3)
C1–C2	1.436(3)	C15–C16	1.448(3)
C1–C4	1.509(3)	C16–C18	1.512(3)
N2–C3	1.347(3)	N3–C14	1.347(3)
N1–C1	1.304(3)	N4–C16	1.302(3)
N2–C3–C2	121.8(2)	N3–C14–C15	122.7(2)
C3–C2–C1	126.2(2)	C14–C15–C16	126.1(2)
N1–C1–C2	121.1(2)	N4–C16–C15	120.7(2)

absence of the downfield N–H resonance in the  $^1\text{H}$  NMR spectrum and the absence of the N–H stretching vibration in the IR spectrum indicate the deprotonation of the ligand to its dianionic form.

Vapor diffusion of pentane into a THF solution gives crystals suitable for X-ray diffraction analysis. The structures of  $\text{mBinLi}_2(\text{THF})_4$  and  $\text{pBinLi}_2(\text{THF})_3$  are shown in Figure 4. Selected bond lengths and angles for  $\text{pBinLi}_2(\text{THF})_3$  are given in Table 2. The crystal structure of the *mBin*-bound complex has four molecules of THF rather than the two evident from integration of  $^1\text{H}$  NMR spectra; however, the NMR spectra were of  $\text{C}_6\text{D}_6$  solutions of crystals that had been exposed to vacuum for hours. It is reasonable to conclude that two of the THF ligands in  $\text{mBinLi}_2(\text{THF})_4$  are held rather weakly. In  $\text{pBinLi}_2(\text{THF})_3$ , on the other hand, the NMR and crystal structure both show three THF ligands to the two lithium ions.

The differences between analogous C–N and C–C bond lengths are much smaller than in the protonated ligand, as expected for resonance delocalization of the charge in the anionic diketiminate unit on each side of the binucleating ligand. In  $\text{mBinLi}_2(\text{THF})_4$  each lithium atom has a pseudotetrahedral geometry with two diketiminate nitrogen atoms and the oxygen atoms of two THF ligands, while in  $\text{pBinLi}_2(\text{THF})_3$  one of the lithium atoms has only one THF ligand and a roughly trigonal-planar geometry. In  $\text{pBinLi}_2(\text{THF})_3$ , the bonds to the four-coordinate lithium atom are significantly longer than those to the three-coordinate lithium atom. The structure of  $\text{mBinLi}_2(\text{THF})_4$  suffers from substantial disorder in the position of the THF ligands and could not be refined to an *R* value below 14%.

The most notable difference between the overall conformations of the lithium salts of  $\text{mBin}^{2-}$  and  $\text{pBin}^{2-}$  is in the orientation of the two (diketiminate)metal units. The molecules are *not* planar, as it appears in a two-dimensional picture. Rather, the crystal structures show that the diketiminate planes are far from the plane of the macrocycle (80–90° for  $\text{mBinLi}_2(\text{THF})_4$ ; 68.76(8) and 11.63(10)° for  $\text{pBinLi}_2(\text{THF})_3$ ). As a result, both metals may lie out of the macrocyclic plane on the same side



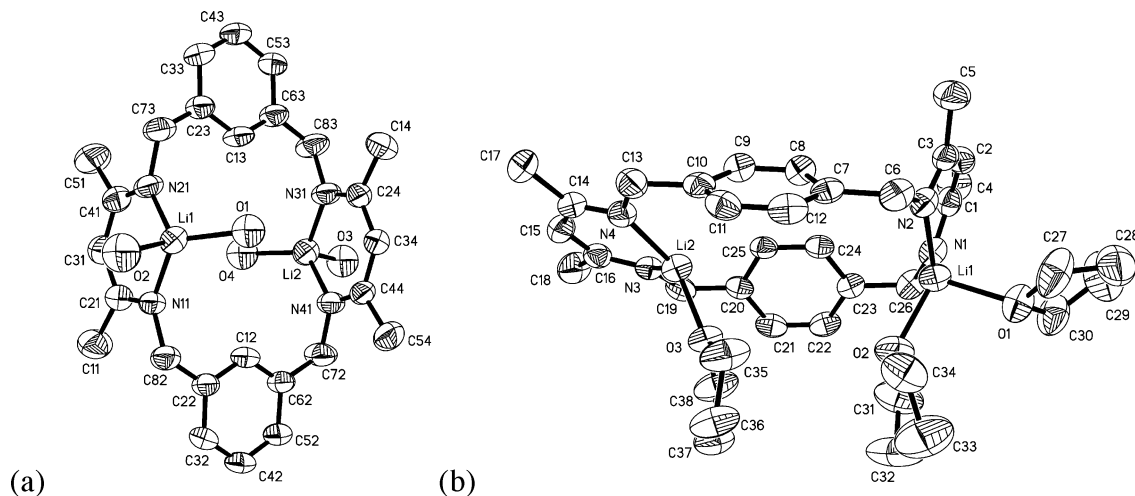


**Figure 4.** Thermal ellipsoid plots of mBinLi<sub>2</sub>(THF)<sub>4</sub> and of pBinLi<sub>2</sub>(THF)<sub>3</sub>, showing 50% probability ellipsoids. Hydrogen atoms are not shown for clarity. The THF ligands in mBinLi<sub>2</sub>(THF)<sub>4</sub> are highly disordered, and only the oxygen atoms are shown.

**Table 2. Selected Bond Lengths (Å) and Angles (deg) for pBinLi<sub>2</sub>(THF)<sub>3</sub> (Figure 4b)<sup>a</sup>**

Li1–N2	1.935(6)	Li1–N1	1.946(6)
Li2–N4	1.921(6)	Li2–N3	1.929(6)
Li1–O1	2.044(6)	Li1–O2	1.981(6)
Li2–O3	1.921(5)		
N1–C1	1.315(4)	N3–C16	1.320(4)
N2–C3	1.316(4)	N4–C14	1.322(4)
C1–C2	1.400(5)	C14–C15	1.397(5)
C2–C3	1.414(5)	C15–C16	1.406(5)
N2–Li1–N1	98.6(2)	O2–Li1–O1	96.6(2)
N4–Li2–N3	98.6(3)	N4–Li2–O3	128.0(3)
N3–Li2–O3	118.9(3)		

<sup>a</sup> The high *R* value for the structure of mBinLi<sub>2</sub>(THF)<sub>4</sub> (Figure 4a) suggests that it does not have reliable metrical parameters.

(the syn conformation; Figure 5, left) or on opposite sides (the anti conformation; Figure 5, right). Despite the similarities in the isomeric Bin<sup>2-</sup> ligands, mBinLi<sub>2</sub>(THF)<sub>4</sub> has the anti conformation, while pBinLi<sub>2</sub>(THF)<sub>3</sub> has the syn conformation (Figure 4). The Li···Li distances are roughly the same (6.05 Å) in the two complexes, despite the smaller macrocyclic ring in the mBin<sup>2-</sup> ligand. This is due to the fact that the diketiminate NCCCN planes are nearly coplanar and anti in mBinLi<sub>2</sub>(THF)<sub>4</sub> and nearly perpendicular (dihedral angle 80.1(1)°) and syn in pBinLi<sub>2</sub>(THF)<sub>3</sub>.

A more careful look at the positions of atoms in these two complexes shows that the signals for the benzylic protons and for the aromatic protons give information about the dynamics of the complexes. In either the syn or anti conformation, the two geminal hydrogen atoms on each benzylic methylene carbon are inequivalent and are expected to appear in the <sup>1</sup>H NMR spectrum as two doublets with a large coupling constant. The coupling pattern, integrations, and general location of peaks are

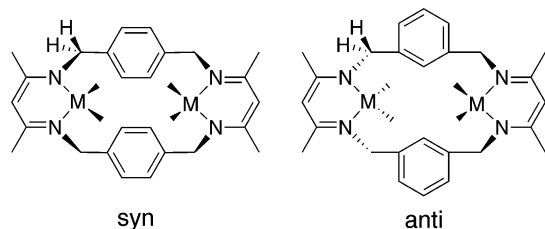


**Figure 5.** Different conformations of metal complexes of the binucleating ligands. In the upper left of each structure are shown the two protons that are diastereotopic in complexes for which interconversion of isomers is slow or absent.

not expected to be different for syn and anti conformers, because each has the same number of symmetry operations, and there are no obvious sources of coupling or NOE that could be exploited to learn the conformation.

In each lithium complex, the benzylic methylene protons resonate as a singlet, which implies a rapid equilibrium between syn and anti conformations on the NMR time scale. Cooling THF-*d*<sub>8</sub> solutions of each lithium complex results in decoalescence of the 8-proton singlet near δ 4.5 ppm, with coalescence temperatures of –11 °C (mBinLi<sub>2</sub>(THF)<sub>n</sub>) and –85 °C (pBinLi<sub>2</sub>(THF)<sub>n</sub>). This phenomenon is due to the slowing of interconversion of the conformers at lower temperature, which makes the geminal benzylic protons chemically distinct. The <sup>1</sup>H NMR spectrum of mBinLi<sub>2</sub>(THF)<sub>n</sub> in THF-*d*<sub>8</sub> at –50 °C (well below the coalescence temperature) has two doublets (*J* = 15 Hz) in this region, indicative of a single conformer, and we assume that this is the anti conformer observed in the X-ray crystal structure. The anti conformers exchange the endo/exo positions of these two protons with the barrier Δ*G*<sup>‡</sup> = 12.9 ± 0.1 kcal/mol.

The low-temperature <sup>1</sup>H NMR spectra of pBinLi<sub>2</sub>(THF)<sub>n</sub> in THF-*d*<sub>8</sub> are more complicated. At –85 °C, all of the peaks decoalesce into two pairs of doublets, with an integration ratio of roughly 2:1. Although the spectra are fairly broad at –100 °C, the region near δ 4.5 ppm clearly has two larger doublets and two smaller doublets, each with coupling constants near 15 Hz (see the Supporting Information). Therefore, the spectra of pBinLi<sub>2</sub>(THF)<sub>n</sub> are indicative of freezing the interconversion of syn and anti conformers, with the barrier Δ*G*<sup>‡</sup> = 8.9 ± 0.3 kcal/mol. In this case, one conformer is only slightly favored over the other.

Note that the four protons on each aromatic ring in the pBin<sup>2-</sup> ligand are expected to split into two sets in either the syn (overall *C*<sub>2v</sub> symmetry; mirror plane through aromatic rings) or the anti (overall *C*<sub>2h</sub> symmetry; *C*<sub>2</sub> axis through aromatic rings) conformation. However, these signals are observed as singlets both above and below the coalescence temperature. This behavior is consistent with the ring rapidly rotating around the two C(methylene)–C(aromatic) bonds on the NMR time scale, even at –100 °C.

Examination of models of both lithium complexes suggests that the syn/anti interconversion requires dissociation of THF ligands (or of diketiminate ligands) from Li. Consistent with rapid THF dissociation, we observe only one THF environment in THF-*d*<sub>8</sub> solutions of each lithium complex by <sup>1</sup>H NMR and

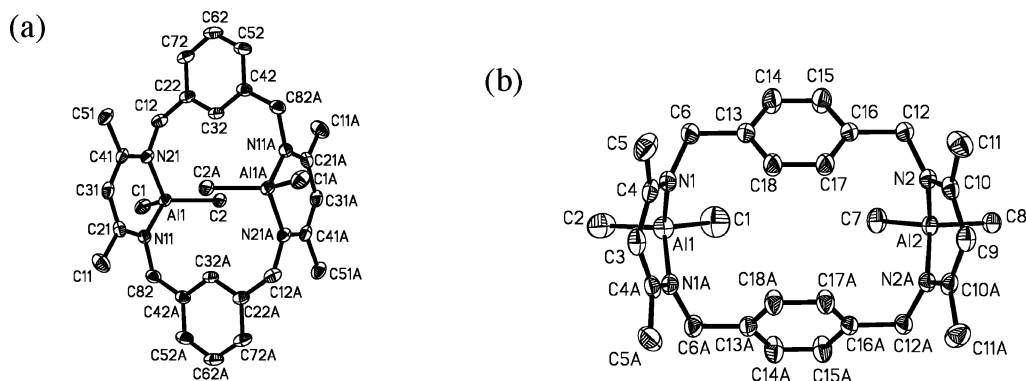


**Figure 6.** Thermal ellipsoid plots of (a)  $m\text{BinAl}_2\text{Me}_4$  and (b)  $p\text{BinAl}_2\text{Me}_4$  showing 50% probability ellipsoids. Hydrogen atoms have been omitted for clarity.

**Table 3. Selected Bond Lengths (Å) and Angles (deg) for  $\text{BinAl}_2\text{Me}_4$  Complexes**

	$m\text{BinAl}_2\text{Me}_4 \cdot (\text{solvent})$	$m\text{BinAl}_2\text{Me}_4$	$p\text{BinAl}_2\text{Me}_4$
N–C (diketiminate)	1.330(2), 1.330(2)	1.333(2), 1.334(2)	1.336(1), 1.334(1)
C–C (diketiminate)	1.402(2), 1.399(2)	1.400(2), 1.404(2)	1.399(1), 1.404(1)
Al–N	1.897(1), 1.899(1)	1.902(1), 1.902(1)	1.9011(9), 1.9025(8)
Al–C	1.971(2), 1.976(2)	1.973(1), 1.902(1)	1.960(2), 1.966(2)
N–Al–N	96.14(6)	96.05(4)	95.36(5), 95.98(5)
C–Al–C	113.64(8)	113.22(6)	115.40(12), 117.44(7)

$^{13}\text{C}\{^1\text{H}\}$  NMR spectroscopy. Therefore, we surmise that the lability of the THF ligands enables rapid interconversion of conformers. Because of the greater size of the macrocycle in the  $p\text{Bin}^{2-}$  ligand, there is more room for the metals to pass by one another, and its dilithium complex can interconvert isomers with a barrier 4 kcal/mol lower than the analogous complex with the  $m\text{Bin}^{2-}$  ligand.

**Aluminum Complexes of the Binucleating Ligands.** Two molar equivalents of trimethylaluminum react with  $m\text{BinH}_2$  and with  $p\text{BinH}_2$  at room temperature in toluene to yield the complexes  $m\text{BinAl}_2\text{Me}_4$  and  $p\text{BinAl}_2\text{Me}_4$ , respectively. Each of these complexes has been characterized by X-ray crystallographic and NMR spectroscopic techniques, which show that each aluminum atom is coordinated by two nitrogen atoms of a diketiminate unit and by two methyl groups. The X-ray crystal structures are shown in Figure 6. Interestingly, two different crystal forms of  $m\text{BinAl}_2\text{Me}_4$  are observed. One contains no solvent of crystallization and a crystallographic inversion center in the center of the molecule. The other crystallizes in a hexagonal lattice with a highly disordered solvent on a special position. The bond distances and angles in  $m\text{BinAl}_2\text{Me}_4$  are extremely similar between the two independent crystallographic determinations (Table 3). The Al–Al distances vary somewhat (5.7630(7) and 5.612(1) Å), but in each case, the NCCC groups are coplanar (enforced by a crystallographic inversion center) and perpendicular to the macrocycle plane (87.53(3) and 89.18°).

The metrical parameters in each diketiminate–aluminum ring are similar to those in the crystallographically characterized mononuclear analogue  $\{\text{HC}(\text{C}(\text{Me})\text{N}(\text{dipp}))_2\}\text{AlMe}_2$ .<sup>27</sup> Comparison to the Cambridge Structural Database<sup>28</sup> shows no exceptional differences from other literature complexes of similar structure. The conformational preferences of the macrocycle differ, depending on which binucleating ligand is present:  $m\text{BinAl}_2\text{Me}_4$  has an anti conformation, while  $p\text{BinAl}_2\text{Me}_4$  has a syn conformation. Note that each of these has the

same conformation observed in the crystal structure of its lithium analogue, suggesting that the conformational preferences are determined by the ligand, not the choice of metal. In contrast to the lithium complexes above, the  $m\text{Bin}^{2-}$  ligand holds the Al atoms closer together (5.6–5.8 Å) than the  $p\text{Bin}^{2-}$  ligand (7.555(1) Å), despite the fact that the metal atoms are on opposite sides of the macrocyclic ring in the  $m\text{Bin}^{2-}$  compound.

Another important difference involves the dynamic behavior of the complexes in solution. In contrast with the lithium salts, the conformation of each aluminum complex is locked: at room temperature the benzylic methylene protons resonate as two doublets with a geminal coupling constant of  $J = 15 \pm 1$  Hz. Consistent with a locked conformation, the two aluminum-bound methyl groups are inequivalent in the  $^1\text{H}$  NMR spectra of each complex, where two resonances are observed upfield of TMS.<sup>29</sup> Because a rapid equilibrium between syn and anti conformations would render these methyl groups equivalent in the NMR spectrum, we conclude that the conformations are locked (at least on the NMR time scale) in each complex. We cannot distinguish syn from anti on the basis of NMR spectroscopy, and so we assume that the crystallographically observed conformation is dominant in solution. Therefore, the crystallographic and NMR data indicate that analogous bis(dimethylaluminum) complexes of  $m\text{Bin}^{2-}$  and  $p\text{Bin}^{2-}$  have different conformations and that these conformations are static on the time scale of the NMR experiment. In  $p\text{BinAl}_2\text{Me}_4$ , all of the aromatic protons resonate at the same frequency, showing that the aromatic rings of the *p*-xylylene linker are again spinning rapidly around the axis defined by the two para substituents.

**Zinc Complexes of the Binucleating Ligands.** Assemblies of cooperating  $\text{Zn}^{2+}$  ions form the active site of many hydrolytic enzymes.<sup>30</sup> Recent attention has come from multimetallic mechanisms for  $\text{Zn}^{2+}$ -catalyzed alternating copolymerization of epoxides with  $\text{CO}_2$ ,<sup>3g</sup> and multimetallic strategies for detecting

(27) Cui, C.; Roesky, H. W.; Schmidt, H.; Noltemeyer, M.; Hao, H.; Cimpoesu, F. *Angew. Chem., Int. Ed.* **2000**, *39*, 4274–4276.

(28) CSD version 5.27, updated August 2006; Allen, F. H. *Acta Crystallogr.* **2002**, *B58*, 380.

(29) In the  $^{13}\text{C}\{^1\text{H}\}$  NMR spectra, the aluminum-bound carbon atoms are shifted upfield and broadened by the quadrupole on  $^{27}\text{Al}$ . Two slightly overlapped signals are seen in  $m\text{BinAl}_2\text{Me}_4$ , and in  $p\text{BinAl}_2\text{Me}_4$  only one signal is seen, presumably because the two signals overlap completely.

biological  $\text{Zn}^{2+}$ .<sup>31</sup> Therefore, dizinc complexes of the Bin ligands are of interest. Diethylzinc reacts with  $\text{mBinH}_2$  and with  $\text{pBinH}_2$  to eliminate ethane at room temperature in toluene. The products are  $\text{mBinZn}_2\text{Et}_2$  and  $\text{pBinZn}_2\text{Et}_2$ , neither of which yielded single crystals suitable for X-ray diffraction analysis. They have been characterized by NMR, IR, and elemental analysis, as well as the crystal structure of a pyridine derivative of  $\text{mBinZn}_2\text{Et}_2$  (see below).

The  $^1\text{H}$  NMR spectrum of  $\text{pBinZn}_2\text{Et}_2$  is indicative of a single conformation, because the geminal benzylic methylene protons are inequivalent (as in the aluminum complexes above). However, as discussed above, the NMR spectra do not distinguish between syn and anti conformations. Given the syn conformations observed in the X-ray crystal structures of the complexes of  $\text{pBin}^{2-}$  with both lithium and aluminum, we speculate (without definitive evidence) that a syn conformation is also dominant for its zinc complex.

Interestingly, the  $^1\text{H}$  NMR spectrum of  $\text{mBinZn}_2\text{Et}_2$  has two sets of protons in a ratio of approximately 2:1. Each set has equivalent relative integrations of Bin and ethyl signals, indicating that both compounds are doubly metalated. The  $^1\text{H}$  NMR spectrum defied assignment in the 4–5 ppm region (see the Supporting Information for the spectrum), suggesting the presence of overlapping peaks with second-order coupling. It is not surprising to find second-order coupling, because the geminal coupling constant in other complexes is  $^2J \approx 15$  Hz, which could be greater than the difference in chemical shifts between coupled protons. The observation of coupling strongly suggests that the two compounds in the  $\text{mBinZn}_2\text{Et}_2$  mixture are conformationally locked on the NMR time scale, and it is most reasonable (based on the analogous lithium and aluminum compounds) to conclude that the two are the syn and anti conformers. The ratio of the two sets of signals in a solution of  $\text{mBinZn}_2\text{Et}_2$  changed from  $\sim 2:1$  to  $\sim 1:1$  upon heating from room temperature to  $90^\circ\text{C}$ , indicating that the conformers interconvert in a longer time regime.

In order to characterize the complexes in more detail, the reactions of  $\text{mBinH}_2$  and of  $\text{pBinH}_2$  with  $\text{ZnEt}_2$  have been performed in the presence of pyridine, yielding white solids characterized as  $\text{mBinZn}_2\text{Et}_2\text{py}_2$  and  $\text{pBinZn}_2\text{Et}_2\text{py}_2$ . These are analogous to dizinc complexes of **1** reported by Lee and co-workers.<sup>19</sup> Excess pyridine does not change the chemical shifts of the peaks for the zinc complex, indicating that the binding of pyridine is weak. Consistent with this idea, repeated washing of the solid with pentane typically removed the pyridine from the complexes, as shown by  $^1\text{H}$  NMR spectroscopy.

Fortunately, we were able to grow a crystal of  $\text{mBinZn}_2\text{Et}_2\text{py}_2$ , which gave the structure shown in Figure 7. Relevant metrical parameters are given in Table 4. The binucleating ligand is in the anti conformation, as seen for the other complexes of the  $\text{mBin}^{2-}$  ligand. The pyridine ligands are on the sides of the zinc atoms furthest from the neighboring zinc, presumably for steric reasons. The geometry at zinc is best described as a trigonal pyramid with the pyridine in the axial position and the ethyl group in an equatorial position. The small influence of the pyridine ligand on the trigonal-planar (diketiminato)ZnEt unit is consistent with the weak binding evident from  $^1\text{H}$  NMR spectra (see above). The two diketiminato ligands are coplanar

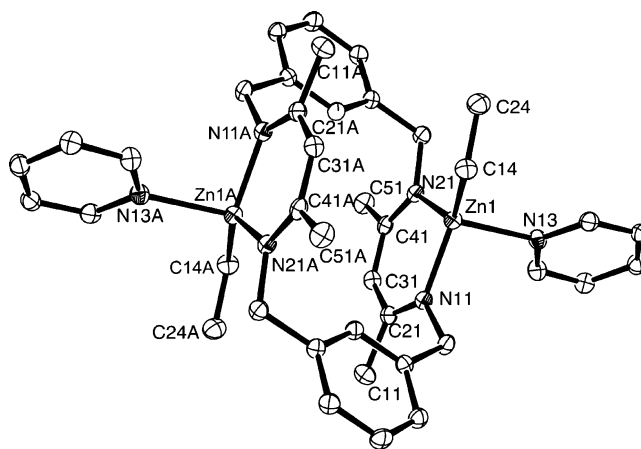


**Figure 7.** Thermal ellipsoid plot of  $\text{mBinZn}_2\text{Et}_2\text{py}_2$  showing 50% probability ellipsoids. Hydrogen atoms have been omitted for clarity.

**Table 4.** Selected Bond Lengths (Å) and Angles (deg) for  $\text{mBinZn}_2\text{Et}_2\text{py}_2$

N11–C21	1.324(3)	N21–C41	1.325(3)
C21–C31	1.411(3)	C31–C41	1.409(3)
Zn1–N11	2.003(2)	Zn1–N21	2.006(2)
Zn1–C14	1.995(2)	Zn1–N13	2.211(2)
C14–Zn1–N11	130.37(8)	C14–Zn1–N21	123.41(8)
N11–Zn1–N21	95.20(7)	C14–Zn1–N13	107.74(8)
N11–Zn1–N13	94.68(7)	N21–Zn1–N13	97.99(7)

(as a result of a crystallographic inversion center) and are perpendicular to the macrocycle ( $89.96(7)^\circ$ ).

The structure of  $\text{mBinZn}_2\text{Et}_2\text{py}_2$  may be compared directly to the ethylzinc–pyridine complex of the binucleating ligand **1** (see above).<sup>19</sup> In that structure, trigonal-pyramidal zinc atoms are also evident. The sum of C14–Zn1–N21, N11–Zn1–N21, and C14–Zn1–N11 angles in  $\text{mBinZn}_2\text{Et}_2\text{py}_2$  is  $349.4^\circ$ , similar to that in the  $\text{Zn}_2\text{Et}_2(\text{py})_2$  complex of **1** ( $346.9^\circ$ ). The Zn–Zn distance in  $\text{mBinZn}_2\text{Et}_2\text{py}_2$  is  $5.2435(9)$  Å; presumably the fact that the apexes of the trigonal pyramids face the outside of the molecule allows the metal atoms to approach each other more closely than in the Li and Al complexes described above. Notice that the Zn–Zn distance is substantially shorter than in the analogous complex of binucleating ligand **1** ( $6.01$  Å, no esd reported).<sup>19</sup>

**Conformational Preferences of the Bin Ligands.** Lee and co-workers have found that zinc(II)– and copper(I)– complexes of the aryl-linked bis-diketiminato ligand **1** display an anti conformation.<sup>19</sup> Complexes of the Bin ligands display more variable conformations. In every case where the conformation of the bimetallic complexes is known from crystallography, the preferred conformation of  $\text{mBin}^{2-}$  complexes is anti and that of  $\text{pBin}^{2-}$  complexes is syn. Because the *m*-xylylene linker constrains the two metal centers to be relatively close, steric effects are the most likely explanation for the anti preference of  $\text{mBin}^{2-}$  complexes. Consistent with this idea, the diketiminato rings are always coplanar with one another, and perpendicular to the macrocycle plane. By adopting the anti conformation, the tetrahedral metal centers are able to avoid placing the non-diketiminato ligands too near one another, which would require destabilizing distortions in the syn conformation. Unfortunately, the anti conformation is not desired for cooperative reactivity between the metal centers, because the available coordination sites on the two metals are far from one another. However, there is some hope for cooperative reactivity, because  $^1\text{H}$  NMR evidence suggests that  $\text{mBinZn}_2\text{Et}_2$  partially populates the syn conformer.

(30) Averill, B. A. Dinuclear Hydrolases. In *Comprehensive Coordination Chemistry II*; McCleverty, J., Meyer, T. J., Eds.; Elsevier: Oxford, U.K., 2004; Vol. 8, pp 641–676.

(31) (a) Nolan, E. M.; Jaworski, J.; Racine, M. E.; Sheng, M.; Lippard, S. J. *Inorg. Chem.* **2006**, *45*, 9748–9757. (b) Nolan, E. M.; Ryu, J. W.; Jaworski, J.; Feazell, R. P.; Sheng, M.; Lippard, S. J. *J. Am. Chem. Soc.* **2006**, *128*, 15517–15528.



It is more difficult to explain why  $p\text{Bin}^{2-}$  complexes prefer the syn conformation. The metals are on the same side of the macrocycle in crystals of  $p\text{Bin}^{2-}$  complexes of lithium and aluminum, suggesting that the syn preference may be a general phenomenon. This contrasts with the case for ligand **1**, which gives the anti conformer in both copper(I) and zinc(II) complexes. It is especially interesting that the crystal structure of  $p\text{BinLi}_2(\text{THF})_3$  clearly shows a preference for the syn conformer despite (presumably) destabilizing nonbonded interactions between the THF ligands on the two lithium centers. This promising feature of  $p\text{Bin}^{2-}$  is tempered by the long ( $>6 \text{ \AA}$ ) distance between two metal centers in crystallographically characterized  $p\text{Bin}^{2-}$  complexes. Future work will aim at ligands with a preference for the syn conformation and a shorter intermetallic distance that encourages cooperative reactions of bimetallic complexes.

## Experimental Section

**General Considerations.** Manipulations were performed under an  $\text{N}_2$  atmosphere by standard Schlenk techniques or in an M. Braun Unilab  $\text{N}_2$ -filled glovebox maintained at or below 1 ppm of  $\text{O}_2$  and  $\text{H}_2\text{O}$ . Glassware was dried at  $150 \text{ }^\circ\text{C}$  overnight. Proton and carbon-13 NMR data were recorded on a Bruker Avance 400 spectrometer (400 MHz for  $^1\text{H}$ ; 101 MHz for  $^{13}\text{C}$ ) at the specified temperature. Chemical shifts ( $\delta$ ) are reported in ppm, relative to residual protiated solvent in benzene- $d_6$  (7.15), THF- $d_8$  (3.58, 1.73), or  $\text{CDCl}_3$  (7.27). IR spectra ( $450\text{--}4000 \text{ cm}^{-1}$ ) were recorded on KBr pellets in a Shimadzu FTIR spectrophotometer (FTIR 8400S), and the spectra are given in the Supporting Information. A total of 32 scans at a  $2 \text{ cm}^{-1}$  resolution were collected in each case. Microanalysis was performed by Desert Analytics (Tucson, AZ). Pentane, diethyl ether, tetrahydrofuran (THF), and toluene were purified by passage through activated alumina and "deoxygenizer" columns from Glass Contour Co. (Laguna Beach, CA). Deuterated benzene and tetrahydrofuran were vacuum-distilled from sodium-benzophenone ketyl into a storage container or directly into the NMR tube. Benzene, ethanol, and ethylene glycol were obtained from Fisher; and *n*-butyllithium (2.5 M in hexane), trimethylaluminum (2 M in hexane), diethylzinc (1.0 M in hexane), 2,4-pentanedione, *p*-toluenesulfonic acid hydrate, *m*-xylylenediamine, and *p*-xylylenediamine were purchased from Aldrich.

**2,4-Pentanedione-2,2-(ethylene glycol) Monoketal.** This procedure was slightly modified from that given in the literature.<sup>32</sup> A mixture of 2,4-pentanedione (20.0 g, 200 mmol), ethylene glycol (12.4 g, 200 mmol), and *p*-toluenesulfonic acid hydrate (43 mg, 0.23  $\mu\text{mol}$ ) was refluxed in benzene (40 mL) for 3 days with azeotropic removal of water. After concentration under reduced pressure at room temperature, distillation under static vacuum (5 mbar,  $120 \text{ }^\circ\text{C}$ ) afforded a colorless liquid: 20.2 g, 70% yield. The presence of substantial impurities in some cases did not affect the purity of subsequent reactions; the  $^1\text{H}$  NMR spectrum of a typical monoketal-containing mixture is given in the Supporting Information. The following peaks correspond to the monoketal.  $^1\text{H}$  NMR ( $\text{C}_6\text{D}_6$ ,  $20 \text{ }^\circ\text{C}$ ): 3.94 (d, 4H,  $-\text{CH}_2\text{CH}_2-$ ), 2.73 (s, 2H,  $-\text{CH}_2-$ ), 2.19 (s, 3H,  $\text{CH}_3$ ), 1.38 (s, 3H,  $\text{CH}_3$ ).

**$m\text{BinH}_2$ .** *m*-Xylylenediamine (425 mg, 3.12 mmol) and 2,4-pentanedione-2,2-(ethylene glycol) monoketal (450 mg, 3.12 mmol) were placed in a resealable tube. The mixture was stirred and heated to  $100 \text{ }^\circ\text{C}$  for 2 h and then cooled to room temperature. Precooled ethanol (ca.  $0 \text{ }^\circ\text{C}$ ) was then added, and the mixture was further stirred at room temperature for 12 h, after which a white solid precipitated. This solid was collected by filtration: 554 mg, 89%. Anal. Found (calcd): C, 77.81 (77.96); H, 7.93 (8.05); N, 14.06

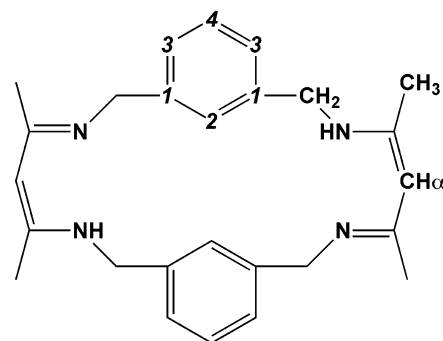


**Figure 8.** Numbering scheme for the *mBin* ligand.

(13.99).  $^1\text{H}$  NMR ( $\text{CDCl}_3$ ,  $21 \text{ }^\circ\text{C}$ , see labeling scheme given in Figure 8): 11.60 (s, 2H, NH), 7.44 (s, 2H, 2-ArCH), 7.19 (t, 2H, 4-ArCH,  $J = 7.2 \text{ Hz}$ ), 7.07 (d, 4H, 3-ArCH,  $J = 7.2 \text{ Hz}$ ), 4.60 (s, 2H,  $\alpha$ -CH), 4.56 (s, 8H,  $\text{CH}_2$ ), 1.92 (s, 12H,  $\text{CH}_3$ ).  $^{13}\text{C}\{^1\text{H}\}$  NMR ( $\text{CDCl}_3$ ,  $21 \text{ }^\circ\text{C}$ ): 161.6 (C=N), 143.2 (aryl), 128.4 (aryl), 126.8 (aryl), 126.3 (aryl), 95.37 ( $\alpha$ -C), 51.19 ( $\text{CH}_2$ ), 19.46 ( $\text{CH}_3$ ). APCI+MS ( $m/z$ ): 401.3  $[\text{M}+\text{H}]^+$ . The IR spectrum is included in the Supporting Information.

**$p\text{BinH}_2$ .** *p*-Xylylenediamine (2.04 g, 15.0 mmol) and 2,4-pentanedione-2,2-(ethylene glycol) monoketal (2.60 g, 18.0 mmol) were placed in a resealable Schlenk flask containing a magnetic stir bar, and the flask was closed. The mixture was then stirred and heated to  $100 \text{ }^\circ\text{C}$  for 30 min. The liquid phase was cooled to room temperature, and precooled ethanol (ca.  $0 \text{ }^\circ\text{C}$ ) was added, causing the immediate precipitation of a white solid that was collected by filtration on a medium frit. Traces of solvent were removed under vacuum overnight. Yield: 1.76 g, 58.7%. Anal. Found (calcd): C, 77.91 (77.96); H, 8.07 (8.05); N, 14.01 (13.99).  $^1\text{H}$  NMR ( $\text{CDCl}_3$ ,  $21 \text{ }^\circ\text{C}$ ): 11.15 (s, 2H, NH), 7.13 (s, 8H, aryl), 4.67 (s, 2H,  $\alpha$ -CH), 4.40 (s, 8H,  $\text{CH}_2$ ), 2.00 (s, 12H,  $\text{CH}_3$ ).  $^{13}\text{C}\{^1\text{H}\}$  NMR (THF- $d_8$ ,  $21 \text{ }^\circ\text{C}$ ): 159.8 (C=N), 138.5 (aryl), 127.3 (aryl), 94.6 ( $\alpha$ -C), 50.5 ( $\text{CH}_2$ ), 19.5 ( $\text{CH}_3$ ). APCI+MS ( $m/z$ ): 401.2  $[\text{M} + \text{H}]^+$ . The IR spectrum is included in the Supporting Information.

**$m\text{BinLi}_2(\text{THF})_2$ .** *n*-Butyllithium (0.80 mL of a 2.5 M solution in hexanes, 2.0 mmol) was added to a stirred solution of  $m\text{BinH}_2$  (400 mg, 1.00 mmol) in THF (25 mL) at room temperature, and stirring was continued for 12 h. The solution was then concentrated to 7 mL and cooled to  $-38 \text{ }^\circ\text{C}$ , to give needles of  $m\text{BinLi}_2\text{THF}$  (389 mg, 68.8%). Anal. Found (calcd) C, 70.14 (73.36); H, 7.87 (8.33); N, 10.07 (10.65).  $^1\text{H}$  NMR ( $\text{C}_6\text{D}_6$ ,  $21 \text{ }^\circ\text{C}$ ): 7.51 (s, 2H, 2-ArCH), 7.04 (t, 2H, 4-ArCH,  $J = 7.2 \text{ Hz}$ ), 6.95 (d, 4H, 3-ArCH,  $J = 7.3 \text{ Hz}$ ), 4.62 (s, 8H,  $\text{CH}_2$ ), 4.48 (s, 2H,  $\alpha$ -CH), 3.28 (t, 8H,  $\alpha$ - $\text{CH}_2$  of THF, 6 Hz), 1.95 (s, 12H,  $\text{CH}_3$ ), 1.21 (m, 8H,  $\beta$ - $\text{CH}_2$  of THF).  $^{13}\text{C}\{^1\text{H}\}$  NMR (THF- $d_8$ ,  $21 \text{ }^\circ\text{C}$ ): 164.3 (C=N), 145.1 (aryl), 126.3 (aryl), 125.3 (aryl), 124.0 (aryl), 92.1 ( $\alpha$ -C), 54.5 ( $\text{CH}_2$ ), 20.4 ( $\text{CH}_3$ ). The IR spectrum is included in the Supporting Information.

**$m\text{BinAl}_2\text{Me}_4$ .** Trimethylaluminum (0.30 mL of a 2 M solution in hexane, 0.60 mmol) was added to a solution of  $m\text{BinH}_2$  (120 mg, 0.30 mmol) in a mixture of toluene (4 mL) and THF (4 mL) at room temperature. After it was stirred for 12 h, the solution was concentrated to 3.5 mL and cooled to  $-38 \text{ }^\circ\text{C}$  to give white crystals (117 mg, 77%). Anal. Found (calcd): C, 69.68 (70.29); H, 8.45 (8.26); N, 10.82 (10.93).  $^1\text{H}$  NMR (THF- $d_8$ ,  $21 \text{ }^\circ\text{C}$ ): 7.67 (s, 2H, 2-ArCH), 7.04 (t, 2H, 4-ArCH,  $J = 7.6 \text{ Hz}$ ), 6.73 (d, 4H, 3-ArCH,  $J = 7.2 \text{ Hz}$ ), 4.58 (s, 2H,  $\alpha$ -CH), 4.52 (d, 4H,  $\text{CH}_2$ ,  $J = 16.4 \text{ Hz}$ ), 4.04 (d, 4H,  $\text{CH}_2$ ,  $J = 16.4 \text{ Hz}$ ), 1.46 (s, 12H,  $\text{CH}_3$ ),  $-0.27$  (s, 6H,  $\text{AlCH}_3$ ),  $-0.45$  (s, 6H,  $\text{AlCH}_3$ ).  $^{13}\text{C}\{^1\text{H}\}$  NMR (THF- $d_8$ ,  $21 \text{ }^\circ\text{C}$ ): 171.5 (C=N), 142.1 (aryl), 128.9 (aryl), 126.2 (aryl), 124.7 (aryl), 98.4 ( $\alpha$ -C), 51.1 (Bn- $\text{CH}_2$ ), 21.8 ( $\text{CH}_3$ ),  $-9.6$  ( $\text{AlCH}_3$ ),  $-10.0$  ( $\text{AlCH}_3$ ). The IR spectrum is included in the Supporting Information.

**$m\text{BinZn}_2\text{Et}_2$ .** Diethylzinc (0.3 mL, 0.3 mmol) was added to a solution of  $m\text{BinH}_2$  (60 mg, 0.15 mmol) in toluene (6 mL) at room

(32) (a) Adkins, H.; Kutz, W.; Coffman, D. C. *J. Am. Chem. Soc.* **1930**, 52, 4391. (b) Dorman, L. C. *Tetrahedron Lett.* **1966**, 459–464.

temperature. After the mixture was stirred overnight, the solvent was removed under vacuum and the product was washed with pentane (6 mL) to produce a powder (65.0 mg, 73.8%). Anal. Found (calcd): C, 61.38 (61.90); H, 7.00 (7.04); N, 9.48 (9.31). The  $^1\text{H}$  NMR of this compound contains two sets of signals (in a 2:1 ratio) that are each consistent with either an anti or a syn conformation.  $^1\text{H}$  NMR ( $\text{C}_6\text{D}_6$ , 21 °C): major set, 7.46–6.86 (m, 8H, ArCH), 4.70–4.61 (m, 6H,  $\alpha$ -CH and  $\text{CH}_2$ ), 4.40 (d, 4H,  $\text{CH}_2$ ,  $J = 15.8$  Hz), 1.70 (s, 12H,  $\text{CH}_3$ ), 1.28 (t, 6H,  $\text{ZnEt}-\text{CH}_3$ ,  $J = 8.0$  Hz), 0.48 (q, 4H,  $\text{ZnEt}-\text{CH}_2$ ,  $J = 8.0$  Hz); minor set, 7.46–6.86 (m, 8H, ArCH), 4.70–4.61 (m, 6H,  $\alpha$ -CH and  $\text{CH}_2$ ), 4.52 (d, 4H,  $\text{CH}_2$ ,  $J = 16.0$  Hz), 1.67 (s, 12H,  $\text{CH}_3$ ), 1.23 (t, 6H,  $\text{ZnEt}-\text{CH}_3$ ,  $J = 8.0$  Hz), 0.32 (q, 4H,  $\text{ZnEt}-\text{CH}_2$ ,  $J = 8.0$  Hz). The IR spectrum is included in the Supporting Information.

**mBinZn<sub>2</sub>Et<sub>2</sub>py<sub>2</sub>.** Diethylzinc (1 mL, 1 mmol) and pyridine (10–20 drops, excess) were added to a solution of mBinH<sub>2</sub> (200 mg, 0.490 mmol) in toluene (10 mL) at room temperature. After it was stirred overnight, the solution was concentrated to 4 mL and cooled to –38 °C, causing the formation of colorless blocklike crystals (230 mg, 61%). Anal. Found (calcd): C, 63.98 (64.43); H, 6.91 (6.76); N, 11.19 (11.27).  $^1\text{H}$  NMR: major set, 8.50 (d, 4H, py *o*-ArCH,  $J = 4.4$  Hz), 7.50–6.87 (m, 8H, ArCH), 6.95 (t, 2H, py *p*-ArCH,  $J = 7.6$  Hz), 6.64 (m, 4H, py *m*-ArCH), 4.80–4.71 (m, 6H,  $\alpha$ -CH and  $-\text{CH}_2$ ), 4.42 (d, 4H,  $-\text{CH}_2$ ,  $J = 16$  Hz), 1.72 (s, 12H,  $\text{CH}_3$ ), 1.31 (t, 6H,  $\text{ZnEt}-\text{CH}_3$ ,  $J = 8$  Hz), 0.50 (q, 4H,  $\text{ZnEt}-\text{CH}_2$ ,  $J = 8$  Hz); minor set, 8.50 (d, 4H, py *o*-ArCH,  $J = 4.4$  Hz), 7.50–6.87 (m, 8H, ArCH), 6.95 (t, 2H, py *p*-ArCH,  $J = 7.6$  Hz), 6.64 (m, 4H, py *m*-ArCH), 4.80–4.71 (m, 6H,  $\alpha$ -CH and  $-\text{CH}_2$ ), 4.52 (d, 2H,  $-\text{CH}_2$ ,  $J = 16$  Hz), 1.69 (s, 12H,  $\text{CH}_3$ ), 1.25 (t, 6H,  $\text{ZnEt}-\text{CH}_3$ ,  $J = 8$  Hz), 0.37 (q, 4H,  $\text{ZnEt}-\text{CH}_2$ ,  $J = 8$  Hz). The IR spectrum is included in the Supporting Information.

**pBinLi<sub>2</sub>(THF)<sub>3</sub>.** *n*-Butyllithium (0.8 mL of a 2.5 M solution in hexanes, 2.0 mmol) was added to pBinH<sub>2</sub> (0.40 g, 1.0 mmol) in THF (6 mL) at room temperature, and the mixture was stirred for 12 h. The solution was concentrated to 2.5 mL and cooled to –38 °C, giving colorless plates (403 mg, 64% yield). Anal. Found (calcd): C, 72.01 (72.59); H, 8.41 (8.66); N, 8.76 (8.91).  $^1\text{H}$  NMR ( $\text{C}_6\text{D}_6$ , 21 °C): 7.35 (s, 8H, ArCH), 4.74 (s, 2H,  $\alpha$ -CH), 4.46 (s,

8H,  $\text{BnCH}_2$ ), 3.27 (m, 12H,  $\alpha$ - $\text{CH}_2$  of THF), 2.10 (s, 12H,  $\text{CH}_3$ ), 1.22 (m, 12H,  $\beta$ - $\text{CH}_2$  of THF).  $^{13}\text{C}\{^1\text{H}\}$  NMR (THF-*d*<sub>8</sub>, 21 °C): 160.7 (C=N), 140.3 (aryl), 124.9 (aryl), 90.2 ( $\alpha$ -C), 51.6 ( $\text{CH}_2$ ), 18.5 ( $\text{CH}_3$ ). The IR spectrum is included in the Supporting Information.

**pBinAl<sub>2</sub>Me<sub>4</sub>.** Trimethylaluminum (0.20 mL of a 2 M solution in hexanes, 0.40 mmol) was added to a solution of pBinH<sub>2</sub> (80 mg, 0.20 mmol) in toluene (8 mL) at room temperature. After it was stirred for 12 h, the solution was concentrated to 4 mL, pentane (6 mL) was layered above the toluene solution, and the vial was cooled to –38 °C, causing the formation of needles (117 mg, 77.0% yield). Anal. Found (calcd): C, 69.76 (70.29); H, 8.68 (8.26); N, 9.57 (10.93).  $^1\text{H}$  NMR ( $\text{C}_6\text{D}_6$ , 21 °C): 6.78 (s, 8H, ArCH), 4.77 (s, 2H,  $\alpha$ -CH), 4.36 (d, 4H,  $\text{CH}_2$ ,  $J = 14.4$  Hz), 4.23 (d, 4H,  $\text{CH}_2$ ,  $J = 14.4$  Hz), 1.55 (s, 12H,  $\text{CH}_3$ ), –0.43 (s, 6H, Al- $\text{CH}_3$ ), –1.11 (s, 6H, Al- $\text{CH}_3$ ).  $^{13}\text{C}\{^1\text{H}\}$  NMR (THF-*d*<sub>8</sub>, 21 °C): 166.3 (C=N), 136.3 (aryl), 126.0 (aryl), 96.0 ( $\alpha$ -C), 47.6 ( $\text{CH}_2$ ), 18.5 ( $\text{CH}_3$ ), –14.6 (Al- $\text{CH}_3$ ). The IR spectrum is included in the Supporting Information.

**pBinZn<sub>2</sub>Et<sub>2</sub>.** Diethylzinc (0.5 mL, 0.5 mmol) was added to a solution of pBinH<sub>2</sub> (100 mg, 0.25 mmol) in toluene (8 mL) at room temperature. After the mixture was stirred for 3 days, the solvent was removed under vacuum and the product was washed with pentane (6 mL) to produce a white powder (108.9 mg, 74.27%). Anal. Found (calcd): C, 61.25 (61.90); H, 6.60 (7.04); N, 9.50 (9.31).  $^1\text{H}$  NMR ( $\text{C}_6\text{D}_6$ , 21 °C): 6.92 (s, 8H, ArCH), 4.62 (s, 2H,  $\alpha$ -CH), 4.56 (d, 4H,  $\text{CH}_2$ ,  $J = 14.8$  Hz), 4.29 (d, 4H,  $\text{CH}_2$ ,  $J = 14.8$  Hz), 1.82 (s, 12H,  $\text{CH}_3$ ), 1.12 (t, 6H,  $\text{ZnEt}-\text{CH}_3$ ,  $J = 8$  Hz), –0.91 (q, 4H,  $\text{ZnEt}-\text{CH}_2$ ,  $J = 8$  Hz). The IR spectrum is included in the Supporting Information.

**Acknowledgment.** This research was supported by the National Institutes of Health (Grant No. GM-065313).

**Supporting Information Available:** CIF files giving crystallographic data and figures giving IR and NMR spectra. This material is available free of charge via the Internet at <http://pubs.acs.org>.

OM0700258